Available online at www.sciencedirect.com
ScienceDirect
Bioorganic & Medicinal Chemistry Letters 18 (2008) 1681–1687
Bioorganic & Medicinal Chemistry Letters

Thiol-based angiotensin-converting enzyme 2 inhibitors: $P^{1'}$ modifications for the exploration of the $S^{1'}$ subsite

David N. Deaton,[a,*] Kevin P. Graham,[b] Jeffrey W. Gross[b] and Aaron B. Miller[c]

[a]*Department of Medicinal Chemistry, GlaxoSmithKline, Research Triangle Park, NC 27709, USA*
[b]*Molecular Discovery Research, Screening & Compound Profiling, GlaxoSmithKline, Upper Providence, PA 19426, USA*
[c]*Molecular Discovery Research, Computational and Structural Chemistry, GlaxoSmithKline, Research Triangle Park, NC 27709, USA*

Received 29 November 2007; revised 10 January 2008; accepted 14 January 2008
Available online 18 January 2008

Abstract—Explorations of the $S^{1'}$ subsite of ACE2 via modifications of the $P^{1'}$ methylene biphenyl moiety of thiol-based metalloprotease inhibitors led to improvements in ACE2 selectivity versus ACE and NEP, while maintaining potent ACE2 inhibition.

Dampening of the renin-angiotensin signaling cascade (RAS) has proven invaluable in the treatment of cardiovascular disease. Drugs that inhibit the M2 family dicarboxymetallopeptidase angiotensin-converting enzyme (ACE, EC 3.4.15.1) or the A1 family aspartic protease renin (EC 3.4.23.15), as well as those that antagonize the 7-transmembrane G protein-coupled angiotensin receptor II (AT_2), improve hypertension. Dual ACE and M13 metalloprotease neutral endopeptidase (neprilysin, NEP, EC 3.4.24.11) inhibition has also been explored for the treatment of high blood pressure. Recently, a new member of the RAS, the M2 family monocarboxymetallopeptidase angiotensin-converting enzyme 2 (ACE2), was identified.[1,2] It is a membrane-associated and secreted metalloprotease, expressed in heart, kidney, testes, intestine, and lung, with highest homology to ACE. ACE2 has been implicated in cardiovascular disease, kidney disease, obesity, and lung disease.[3–5]

Angiotensin I and the AT_1 & AT_2 receptor agonist angiotensin II are substrates for ACE2, which converts them into angiotensin (1-9) and the *mas* receptor agonist angiotensin (1-7), respectively, revealing a role for ACE2 in RAS regulation. Moreover, ACE2 (−/−) mice studies have revealed roles for this protease in cardiac contractility,[6] angiotensin II-induced hypertension,[7] and heart failure.[8] Furthermore, male ACE2 (−/Y) mice, but not female ACE2 (−/−) mice, also develop glomerulosclerosis of the kidneys,[9] but ACE2's exact role in the renin-angiotensin system (RAS) still needs to be clarified. In addition, ACE2 (−/−) mice are resistant to weight gain on a high fat diet.[10] Finally, ACE2 is the primary receptor for the severe acute respiratory syndrome (SARS) corona virus's entry into cells.[11] ACE2 (−/−) mice resist SARS corona virus infection.[12] Because of limited space, the authors refer the interested reader to a recent review by Hamming et al. for a more comprehensive summary of the physiology and pathology of ACE2.[13]

With the many putative roles of ACE2, small molecule modulators of this enzyme's activity could be utilized to help further define the physiological functions of this enzyme. Although small molecule inducers of proteases are difficult to discover, ACE2 activators could provide further insight into the functions of ACE2 and the substrates it processes. Similarly, inhibitors could also shed more light on the roles of ACE2 and the proteins/peptides it activates/degrades.

Efforts to discover ACE2 inhibitors have recently been disclosed. Millennium Pharmaceutical researchers reported the discovery of a reversible, subnanomolar ACE2 inhibitor MLN-4760 (IC_{50} = 0.44 nM), derived from a micromolar lead.[14] In addition, Dyax researchers identified micromolar peptide inhibitors of ACE2 using a phage display library approach, including the 29 amino acid cyclic peptide DX600 (IC_{50} = 10 nM).[15]

Keywords: Angiotensin-converting enzyme 2; Metalloproteases; Protease inhibitors; Thiols.
* Corresponding author. Tel.: +1 919 483 6270; fax: +1 919 315 0430; e-mail: david.n.deaton@gsk.com

0960-894X/$ - see front matter © 2008 Elsevier Ltd. All rights reserved.
doi:10.1016/j.bmcl.2008.01.046

Furthermore, a pharmacophore-based virtual screening approach of commercial databases identified several micromolar ACE2 inhibitors. The best inhibitor was 4S-16659 (IC_{50} = 62,000 nM).[16] Finally, researchers at the University of Florida also utilized a virtual screening exercise of the NCI database to identify *N*-(2-aminoethyl)-1 aziridine-ethanamine (NAAE) (IC_{50} = 57,000 nM) as an irreversible inhibitor of ACE2.[17]

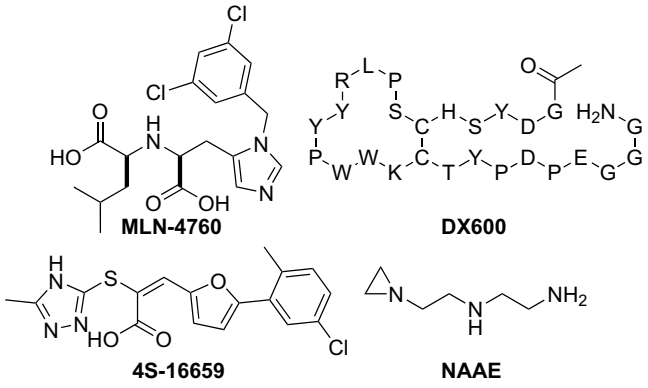

Recently, employing a directed screen of a set of metalloprotease inhibitors from the GlaxoSmithKline compound collection, GSK researchers reported the identification of a known ACE/NEP inhibitor as a potent inhibitor of the zinc metalloprotease ACE2.[18] Structure/activity studies of the S^1 subsite of ACE2 led to the identification of P^1 modified thiol acid **1a** as a more potent ACE2 inhibitor ($K_{i\ App}$ = 1.5 nM) with improved selectivity versus ACE ($K_{i\ App}$ = 490 nM) and NEP ($K_{i\ App}$ = 27 nM). It also inhibits the M14 metalloprotease carboxypeptidase A1 (CpA, EC 3.4.17.1, $K_{i\ App}$= 11,000 nM). Speculating that selectivity could be improved by exploiting potential differences in the $S^{1'}$ subsites of ACE, ACE2, and NEP, the structure–activity relationships of the $P^{1'}$ position of inhibitor **1a** were explored, with the goal of maintaining potency and reducing ACE and NEP inhibitory activity.

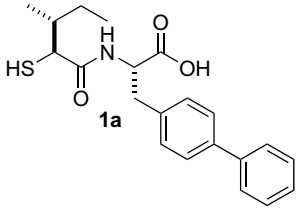

The thiol analogs **1a**–**1t** were prepared as depicted in Scheme 1. The amine hydrochlorides **2a**–**2t** were coupled to the acid **3**, after its in situ activation to the aza-

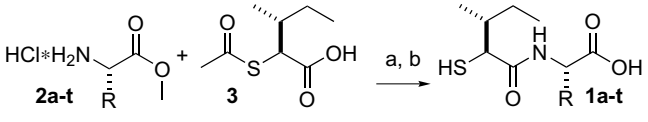

Scheme 1. Reagents and conditions: (a) EDC, HOAt, *i*-Pr_2NEt, CH_2Cl_2, rt, 39–76%; (b) LiOH·H_2O, THF, H_2O, rt, 56–94%.

hydroxybenzotriazole ester via the carbodiimide, to produce the fully protected amides. Then, hydrolysis of the thioacetate and methyl ester with lithium hydroxide afforded the thiol acids **1a**–**1t**.[19]

Amine hydrochlorides **2a**–**2g**, **2l**, and **2o** were commercially available. The remaining amine hydrochlorides **2h**–**2k**, **2m**–**2n**, and **2p**–**2t** were prepared as depicted in Scheme 2. The commercially available amino acids **4a**–**4b** were converted to their corresponding methyl esters with thionyl chloride and methanol at reflux. Then, the resulting amine hydrochlorides were protected as the *tert*-butyl carbamates **5a**–**5b** with di-*tert*-butyl dicarbonate. A Suzuki cross coupling of the *o*-bromide **5a** (X = Br) with phenyl boronic acid afforded the *o*-biphenyl derivative **6a**. Acid catalyzed cleavage of the carbamate gave the *o*-biphenyl amine hydrochloride **2h**. The *m*-phenol **5b** (X = OH) was converted into the triflate with trifluoromethanesulfonic anhydride, and then coupled via the Suzuki protocol to phenyl boronic acid, providing the fully protected *m*-biphenyl derivative **6b**. Subsequent hydrolysis of the amine masking group gave the *m*-biphenyl amine hydrochloride **2i**. The *o*-bromide **5a** (X = Br) was converted into the *o*-phenol **5c** (X = OH) via palladium-mediated transformation of the bromide into a boronate ester, and then oxidation of the boronate to the phenol with hydrogen peroxide. Employing a modified Ullmann ether synthesis protocol, the *o*-phenol **5c** and *m*-phenol **5b** were coupled with phenyl boronic acid to afford the *o*- and *m*-diaryl ethers

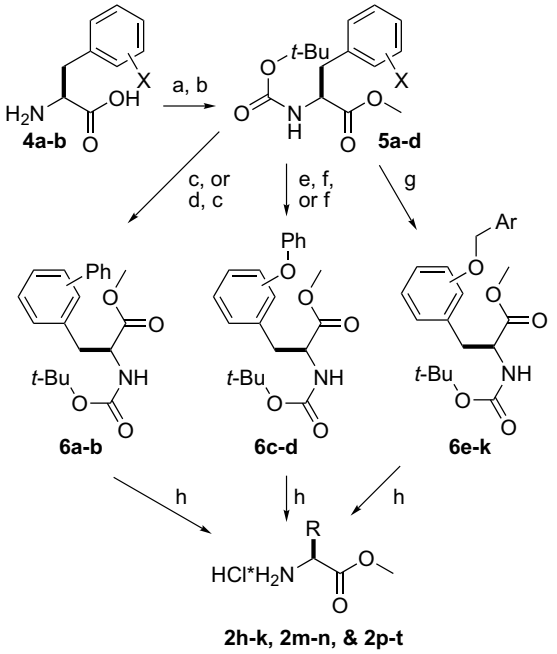

Scheme 2. Reagents and conditions: (a) $SOCl_2$, MeOH, ↑↓, 95–99%; (b) Boc_2O, *i*-Pr_2NEt, CH_2Cl_2, 0 °C to rt, 97–99%; (c) X = Br or OTf, $PhB(OH)_2$, $Pd(PPh_3)_4$, K_2CO_3, PhMe, 90 °C, 41–57%; (d) X = OH, Tf_2O, pyridine, CH_2Cl_2, 0 °C to rt, 88%; (e) X = Br, $PdCl_2$(dppf), bis(pinacolato)diborane, KOAc, DMF, 80 °C; 30% H_2O_2 (aq), MeOH, 44%; (f) X = OH, $Cu(OAc)_2$, $PhB(OH)_2$, pyridine, powdered 4 Å molecular sieves, CH_2Cl_2, rt, 70–96%; (g) X = OH, $ArCH_2Br$, K_2CO_3, acetone, rt, 71–99%; (h) HCl, MeOH, 91–98%.

6c and **6d**. Acidic uncloaking of the *tert*-butyl carbonyl protecting group, then produced the phenyl ethers **2j** and **2k**. Finally, utilizing the Williamson ether synthesis, the *o*-phenol **5c**, the *m*-phenol **5b**, and the commercially available *p*-phenol **5d** were alkylated with various benzyl bromides to give the fully masked benzyl aryl ethers **6e**–**6k**. Then, unmasking of the carbamates afforded the amine hydrochlorides **2m**–**2n** and **2p**–**2t**.

The structure/activity relationships of $P^{1'}$ analogs are depicted in Table 1. Complete removal of the $P^{1'}$ substituent as in analog **1b** resulted in a large decrease in ACE2 ($K_{i\,App}$ = 90 nM) and NEP ($K_{i\,App}$ = 5100 nM) inhibitory activity. The potential reduction in van der Waals interactions from the absence of a $P^{1'}$ side chain as well as the entropic gain from increased rotational freedom of the acid could account for this decrease in potency. In contrast, this change had little affect on ACE ($K_{i\ App}$ = 250 nM) or CpA ($K_{i\ App}$ = 35,000 nM). The alanine-derived analog **1c** (ACE2 $K_{i\ App}$ = 14 nM, NEP $K_{i\ App}$ = 950 nM) decreases rotational freedom and recovers some of the ACE2 inhibitory activity lost upon removal of the $P^{1'}$ group, while not dramatically changing the activity versus ACE ($K_{i\ App}$ = 180 nM) or CpA ($K_{i\ App}$ = 11,000 nM). The phenylalanine and tyrosine derivatives **1d** ($K_{i\,App}$ = 1.5 nM) and **1e** ($K_{i\,App}$ = 1.3 nM) were equipotent ACE2 inhibitors to the methylene *p*-biphenyl analog **1a** with similar ACE (**1d** $K_{i\ App}$ = 570 nM, **1e** $K_{i\ App}$ = 410 nM) and NEP (**1d** $K_{i\ App}$ = 35nM, **1e** $K_{i\ App}$ = 75 nM) activities as well. In contrast to **1a**, the benzyl derivatives **1d** and **1e** were >10-fold more potent inhibitors of CpA (**1d** $K_{i\,App}$ = 530 nM, **1e** $K_{i\ App}$ = 350 nM). Since many good CpA substrates contain $P^{1'}$ phenylalanine residues, this increase in CpA inhibition for **1d** and **1e** is not surprising.

It was decided to explore other bulky $P^{1'}$ substituents with the goal of further improving on the potency and/or selectivity of analog **1a**, since the bulky methylene biphenyl $P^{1'}$ moiety is readily accommodated by the ACE2 enzyme, implying a large $S^{1'}$ subsite. Although the α-methylene naphthyl and the β-methylene naphthyl derivatives **1f** ($K_{i\ App}$ = 2.2 nM) and **1g** ($K_{i\ App}$ = 2.4 nM) were also potent ACE2 inhibitors with >100-fold selectivity versus ACE (**1f** $K_{i\ App}$= 1,800 nM, **1g** $K_{i\ App}$ = 310 nM) and CpA (**1f** $K_{i\ App}$= 3600 nM, **1g** $K_{i\ App}$ = 7200 nM), they still retained substantial inhibitory activity against NEP (**1f** $K_{i\ App}$ = 12 nM, **1g** $K_{i\ App}$ = 46 nM).

In contrast to the *p*-phenyl phenylalanine derivative **1a**, the *o*-phenyl phenylalanine analog **1h** ($K_{i\ App}$ = 37 nM) was an order of magnitude less potent ACE2 inhibitor. This substitution also reduced ACE ($K_{i\ App}$ = 20,000 nM) and NEP ($K_{i\ App}$ = 190 nM) inhibition, while not altering CpA potency ($K_{i\ App}$ = 9900 nM). In contrast to **1h**, the methylene *m*-biphenyl derivative **1i** ($K_{i\ App}$ = 2.2 nM) was an equipotent ACE2 inhibitor to the *p*-derivative **1a**, despite branching from the phenyl moiety at a different angle, but it offered no clear selectivity advantages over ACE ($K_{i\ App}$ = 1000 nM), NEP ($K_{i\ App}$ = 19 nM), or CpA ($K_{i\ App}$ = 5000 nM) versus **1a**.

Although the large biphenyl derivatives were fairly rigid, they were tolerated in the $S^{1'}$ subsite of ACE2. Thus, bulkier $P^{1'}$ groups were explored. The *o*-, *m*-, and *p*-phenoxy phenylalanine derivatives **1j** ($K_{i\ App}$ = 0.90 nM), **1k** ($K_{i\ App}$ = 5.8 nM), and **1l** ($K_{i\ App}$ = 2.2 nM) retained good potency for ACE2 inhibition and >100-fold selectivity versus ACE (**1j** $K_{i\ App}$ = 5000 nM, **1k** $K_{i\ App}$ = 1100 nM, **1l** $K_{i\ App}$ = 250 nM) and CpA (**1j** $K_{i\ App}$ = 2300 nM, **1k** $K_{i\ App}$ = 14,000 nM, **1l** $K_{i\ App}$ = 8900 nM), despite altered branching termini. In contrast, their NEP selectivity differed. The *o*-phenyloxy analog **1j** ($K_{i\ App}$ = 180 nM) was 200-fold selective versus NEP, while the *m*-phenoxy analog **1k** ($K_{i\ App}$ = 79 nM) and the *p*-phenoxy analog **1l** ($K_{i\ App}$ = 10 nM) were 14-fold and 5-fold NEP selective, respectively.

Surprisingly, the extended *o*-, *m*-, and *p*-benzyloxy phenylalanine derivatives **1m** ($K_{i\ App}$ = 6.0 nM), **1n** ($K_{i\ App}$ = 2.4 nM), and **1o** ($K_{i\ App}$ = 2.7 nM) were also well tolerated in the $S^{1'}$ subsite of ACE2. In addition, they maintained good selectivity versus ACE (**1m** $K_{i\ App}$ = 770 nM, **1n** $K_{i\ App}$ = 750 nM, **1o** $K_{i\ App}$ = 570 nM) and CpA (**1m** $K_{i\ App}$ = 1600 nM, **1n** $K_{i\ App}$ = 5000 nM, **1o** $K_{i\ App}$ = 4600 nM). In contrast to the phenyloxy analogs, the *p*-benzyl analog **1o** ($K_{i\ App}$ = 300 nM) was quite selective versus NEP (110-fold), while the *o*-benzyloxy analog **1m** ($K_{i\ App}$ = 120 nM) and the *m*-benzyloxy analog **1n** ($K_{i\ App}$ = 37 nM) were less selective (20-fold and 15-fold, respectively).

Both the methylene *o*-phenoxyphenyl derivative **1j** and the methylene *p*-benzyloxyphenyl analog **1o** are potent and selective ACE2 inhibitors, but the latter inhibitor is readily derived from the cheap natural amino acid tyrosine. Therefore, fluorinated derivatives of inhibitor **1o** were prepared with the goal of maintaining potency and selectivity, while blocking potential metabolic sites of the naked phenyl ring. It was hoped that electron withdrawing groups would not only sterically impede metabolism, but also electronically deactivate the aryl ring to oxidation. The mono- and difluoro analogs **1p** ($K_{i\ App}$ = 2.5 nM), **1q** ($K_{i\ App}$ = 2.0 nM), and **1r** ($K_{i\ App}$ = 0.85 nM) were potent ACE2 inhibitors with good selectivity. The 3,4-difluorobenzyl tyrosine derivative **1r** was the most selective analog with >750-fold separation in $K_{i\ App}$s between ACE2 and ACE ($K_{i\ App}$ = 1800 nM), NEP ($K_{i\ App}$ = 640 nM), and CpA ($K_{i\ App}$ = 3300 nM). In contrast to the ACE2 inhibition of the fluoro derivatives **1p**–**1r**, the larger trifluoromethyl derivatives **1s** ($K_{i\ App}$ = 35 nM) and **1t** ($K_{i\ App}$ = 84 nM) were substantially less potent ACE2 inhibitors. Likely, these larger $P^{1'}$ substituents clash with the residues that make up the $S^{1'}$ subsite.

In vitro drug metabolism and pharmacokinetic assays were performed to help predict *in vivo* oral bioavailabilities and pharmacokinetics of the thiols. Although these inhibitors conform to Lipinski's Rule of 5, the Madin-Darby canine kidney (MDCK) assay revealed that this inhibitor class had poor to moderate passive cell permeabilities (P_{APP} = 5–47 nm/s).[20] Since many dipeptides are absorbed by active transport mechanisms, representative thiol-based inhibitors were dosed orally in the rat

Table 1. Inhibition of human ACE2, ACE, NEP, and CpA

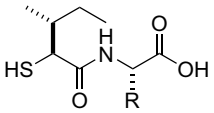

1a-t

#	R	ACE2 $K_{i\ App}$[a] (nM)	ACE $K_{i\ App}$[b] (nM)	NEP $K_{i\ App}$[c] (nM)	CpA $K_{i\ App}$[d] (nM)
1a	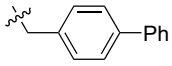	1.5	490	27	11,000
1b	H	90	250	5100	35,000
1c	Me	14	180	950	11,000
1d	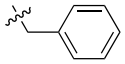	1.5	570	35	530
1e		1.3	410	75	350
1f	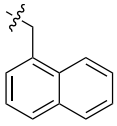	2.2	1800	12	3600
1g	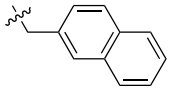	2.4	310	46	7200
1h	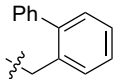	37	20,000	190	9900
1i	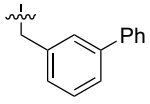	2.2	1000	19	5000
1j	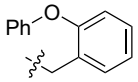	0.90	5000	180	2300
1k	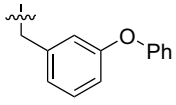	5.8	1100	79	14,000
1l	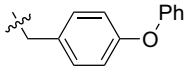	2.2	250	10	8900
1m	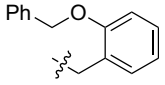	6.0	770	120	1600
1n	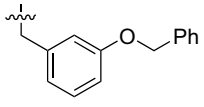	2.4	750	37	5000
1o	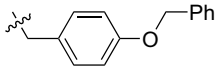	2.7	570	300	4600

Table 1 (*continued*)

#	R	ACE2 $K_{i\ App}$[a] (nM)	ACE $K_{i\ App}$[b] (nM)	NEP $K_{i\ App}$[c] (nM)	CpA $K_{i\ App}$[d] (nM)
1p	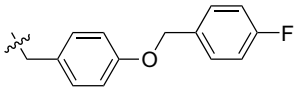	2.5	4000	180	16,000
1q	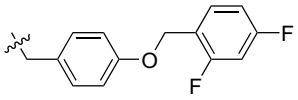	2.0	950	75	1900
1r	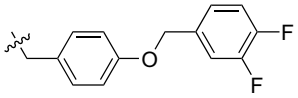	0.85	1800	640	3300
1s	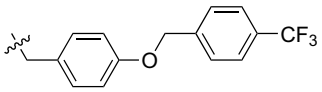	35	2600	1500	4600
1t	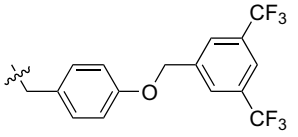	84	25,000	11,000	11,000

[a] Inhibition of recombinant human ACE2 activity in a fluorescence assay using 0.4 nM ACE2, 30 μM MCA-Tyr-Val-Ala-Asp-Ala-Pro-Lys(DNP)-OH as substrate in 1 μM $Zn(OAc)_2$, 100 μM TCEP, 50 mM Hepes, 300 μM CHAPS, and 300 mM NaCl at pH = 7.5. The $K_{i\ App}$ values are means of at least two inhibition assays.

[b] Inhibition of recombinant human ACE activity in a fluorescence assay using 0.5 nM ACE, 10 μM MCA-Ala-Ser-Asp-Lys-Dap(DNP)-OH as substrate in 1 μM $Zn(OAc)_2$, 100 μM TCEP, 50 mM Hepes, 300 μM CHAPS, and 300 mM NaCl at pH = 7.5. The $K_{i\ App}$ values are means of at least two inhibition assays.

[c] Inhibition of recombinant human NEP activity in a fluorescence assay using 0.15 nM NEP, 2 μM FAM-Gly-Pro-Leu-Gly-Leu-Phe-Ala-Arg-Lys(TAMRA)-NH_2 as substrate in 1 μM $Zn(OAc)_2$, 100 μM TCEP, 50 mM Hepes, 300 μM CHAPS, and 300 mM NaCl at pH = 7.5. The $K_{i\ App}$ values are means of at least two inhibition assays.

[d] Inhibition of recombinant human CpA activity in a fluorescence assay using 37 nM CpA, 30 μM Abz-Gly-Gly-Nph-OH as substrate in 1 μM $Zn(OAc)_2$, 100 μM TCEP, 50 mM Hepes, 300 μM CHAPS, and 300 mM NaCl at pH = 7.5. The $K_{i\ App}$ values are means of at least two inhibition assays.

despite their poor predicted cell permeation, but they had limited absorption ($F < 10\%$) in agreement with the MDCK assay.

A model[21,22] of the thiol **1r** docked into the active site of ACE2 based on the recent Millennium X-ray crystal structure[23] is shown in Figure 1. It provides insight into the $P^{1'}$ SAR of the thiol series. The terminal carboxylate of the inhibitor accepts hydrogen bonds from the imidazoles of ^{345}His and ^{505}His and forms a salt bridge to the guanidine of ^{273}Arg. Also, the amide nitrogen of the inhibitor donates a hydrogen atom to the carbonyl of ^{346}Pro, while the amide carbonyl accepts a hydrogen atom from ^{515}Tyr. Moreover, in addition to its normal ACE2 ligands, the imidazole nitrogens of ^{374}His and ^{378}His and the carboxylate of ^{402}Glu, the active site zinc coordinates the thiol of the inhibitor. Furthermore, the P^1 *sec*-butyl group of the inhibitor forms van der Waals interactions with the S^1 pocket composed of ^{347}Thr, ^{504}Phe, ^{510}Tyr, and ^{514}Arg. The greasy $P^{1'}$ 3,4-difluorobenzyltyrosine side chain of **1r** forms significant lipophilic interactions with the quite large $S^{1'}$ channel composed of the lengthwise canal between the two subdomains, including residues ^{274}Phe, ^{445}Thr, ^{406}Glu,

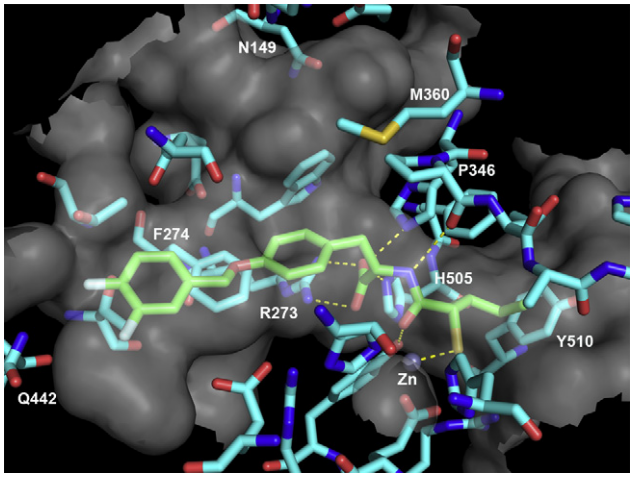

Figure 1. A model of the thiol compound **1r** bound to the active site of ACE2 based on the X-ray co-crystal structure of MLN-4760 bound to ACE2 (PDB code 1R4L). The ACE2 carbons are colored cyan with inhibitor **1r** carbons colored green. The semi-transparent gray surface represents the molecular surface, while hydrogen bonds are depicted as yellow dashed lines. Several residues were removed for visual clarity. This figure was generated using PYMOL version 1.0 (Delano Scientific, www.pymol.org).

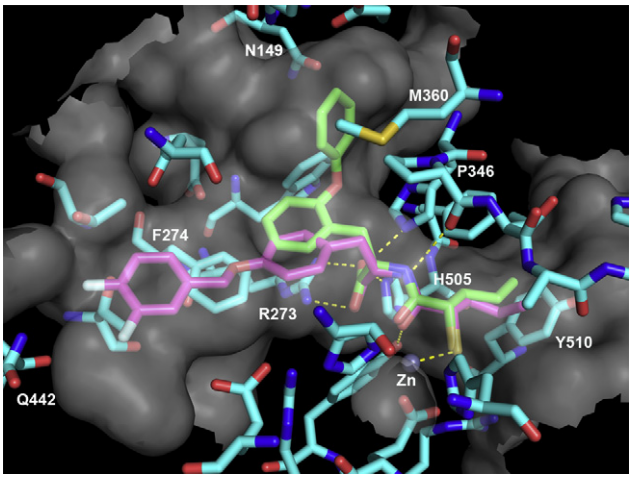

Figure 2. A comparison of the models of the thiol compounds **1j** (carbons colored in green) and **1r** (carbons colored in magenta) bound to the active site of ACE2 (carbons colored in cyan) based on the X-ray co-crystal structure (PDB code 1R4L). The semi-transparent gray surface represents the molecular surface, while hydrogen bonds are depicted as yellow dashed lines. Several residues were removed for visual clarity. This figure was generated using PYMOL version 1.00.

^{409}Ser, ^{370}Leu, ^{371}Thr, ^{276}Thr and extending over to ^{441}Lys and ^{442}Gln. Although several residues in this pocket are hydrophilic, most of the polar groups are either involved in hydrogen bonds with other enzyme residues or oriented away from the $S^{1'}$ pocket, maintaining the lipophilic nature of this subsite. Based on this model, the 3,4-difluorobenzyl portion of the $P^{1'}$ substituent is hypothesized to occupy a different part of this large pocket than the $P^{1'}$ side chain of the carboxyl inhibitor MLN-4760 co-crystallized in 1R4L.

In contrast, as shown in Figure 2, a model[21,22] of the thiol **1j** docked into the active site of ACE2 revealed that the *o*-phenyloxy $P^{1'}$ group occupies a different part of the $S^{1'}$ subsite than the 3,4-difluorobenzyl substituent of analog **1r**. The *o*-phenyloxy $P^{1'}$ moiety fits into a portion of the $S^{1'}$ subsite composed of ^{360}Met, ^{346}Pro, ^{362}Thr, ^{271}Trp, ^{368}Asp, ^{371}Thr, ^{127}Tyr, ^{144}Leu, ^{149}Asn, ^{363}Lys, and ^{269}Asp, and the disulfide pair of ^{344}Cys and ^{361}Cys. Thus, the *o*-phenyloxy $P^{1'}$ moiety of **1j** binds similarly to the $P^{1'}$ side chain of the Millennium carboxyl inhibitor MLN-4760 co-crystallized in 1R4L. The other interactions of inhibitor **1j** are similar to those for analog **1r**. Thus, these two models help explain the divergent $P^{1'}$ SAR, since the very large, forked $S^{1'}$ subsite can tolerate substituents with different branching points.

In summary, variation of substituents at the $P^{1'}$ position in a series of α-thiol amide-based inhibitors of ACE2 resulted in the discovery of potent inhibitors with good ACE and NEP selectivity. Inhibitors containing *p*-methylene aryl tyrosine $P^{1'}$ moieties like **1o**, **1p**, and **1r** were some of the more selective ACE2 inhibitors. In addition, *o*-phenyloxy phenylalanine analog **1j** was also a potent and selective ACE2 inhibitor. These analogs may prove useful in further defining the roles ACE2 plays in the RAS cascade.

Acknowledgments

The authors thank Andrea Epperly, Chuck Poole, and Jo Salisbury for the pharmacokinetic studies.

Supplementary data

Supplementary data associated with this article can be found, in the online version, at doi:10.1016/j.bmcl.2008.01.046.

References and notes

1. Donoghue, M.; Hsieh, F.; Baronas, E.; Godbout, K.; Gosselin, M.; Stagliano, N.; Donovan, M.; Woolf, B.; Robison, K.; Jeyaseelan, R.; Breitbart, R. E.; Acton, S. *Circ. Res.* **2000**, *87*, e1.
2. Tipnis, S. R.; Hooper, N. M.; Hyde, R.; Karran, E.; Christie, G.; Turner, A. J. *J. Biol. Chem.* **2000**, *275*, 33238.
3. Danilczyk, U.; Penninger, J. M. *Circ. Res.* **2006**, *98*, 463.
4. Kuba, K.; Imai, Y.; Penninger, J. M. *Curr. Opin. Pharm.* **2006**, *6*, 271.
5. Tallant, E. A.; Ferrario, C. M.; Gallagher, P. E. *Future Cardiol.* **2006**, *2*, 335.
6. Crackower, M. A.; Sarao, R.; Oudit, G. Y.; Yagil, C.; Kozieradzki, I.; Scanga, S. E.; Oliveira-dos-Santos, A. J.; da Costa, J.; Zhang, L.; Pei, Y.; Scholey, J.; Ferrario, C. M.; Manoukian, A. S.; Chappell, M. C.; Backx, P. H.; Yagil, Y.; Penninger, J. M. *Nature* **2002**, *417*, 822.
7. Gurley, S. B.; Allred, A.; Le, T. H.; Griffiths, R.; Mao, L.; Philip, N.; Haystead, T. A.; Donoghue, M.; Breitbart, R. E.; Acton, S. L.; Rockman, H. A.; Coffman, T. M. *J. Clin. Invest.* **2006**, *116*, 2218.
8. Yamamoto, K.; Ohishi, M.; Katsuya, T.; Ito, N.; Ikushima, M.; Kaibe, M.; Tatara, Y.; Shiota, A.; Sugano, S.; Takeda, S.; Rakugi, H.; Ogihara, T. *Hypertension* **2006**, *47*, 718.
9. Oudit, G. Y.; Herzenberg, A. M.; Kassiri, Z.; Wong, D.; Reich, H.; Khokha, R.; Crackower, M. A.; Backx, P. H.; Penninger, J. M.; Scholey, J. W. *Am. J. Pathol.* **2006**, *168*, 1808.
10. Acton, S. L.; Ocain, T. D.; Gould, A. E.; Dales, N. A.; Guan, B.; Brown, J. A.; Patane, M.; Kadambi, V. J.; Solomon, M.; Stricker-Krongrad, A. *PCT Int. Appl.* WO 039997, **2002**; *Chem. Abstr*. **2002**, *136*, 402027.
11. Li, W.; Moore, M. J.; Vasilieva, N.; Sui, J.; Wong, S. K.; Berne, M. A.; Somasundaran, M.; Sullivan, J. L.; Luzuriaga, K.; Greenough, T. C.; Choe, H.; Farzan, M. *Nature* **2003**, *426*, 450.
12. Kuba, K.; Imai, Y.; Rao, S.; Gao, H.; Guo, F.; Guan, B.; Huan, Y.; Yang, P.; Zhang, Y.; Deng, W.; Bao, L.; Zhang, B.; Liu, G.; Wang, Z.; Chappell, M.; Liu, Y.; Zheng, D.; Leibbrandt, A.; Wada, T.; Slutsky, A. S.; Liu, D.; Qin, C.; Jiang, C.; Penninger, J. M. *Nat. Med.* **2005**, *11*, 875.
13. Hamming, I.; Cooper, M. E.; Haagmans, B. L.; Hooper, N. M.; Korstanje, R.; Osterhaus, A. D. M. E.; Timens, W.; Tumer, A. J.; Navis, G.; van Goor, H. *J. Pathol.* **2007**, *212*, 1.
14. Dales, N. A.; Gould, A. E.; Brown, J. A.; Calderwood, E. F.; Guan, B.; Minor, C. A.; Gavin, J. M.; Hales, P.; Kaushik, V. K.; Stewart, M.; Tummino, P. J.; Vickers, C. S.; Ocain, T. D.; Patane, M. A. *J. Am. Chem. Soc.* **2002**, *124*, 11852.
15. Huang, L.; Sexton, D. J.; Skogerson, K.; Devlin, M.; Smith, R.; Sanyal, I.; Parry, T.; Kent, R.; Enright, J.; Wu,

Q.; Conley, G.; DeOliveira, D.; Morganelli, L.; Ducar, M.; Wescott, C. R.; Ladner, R. C. *J. Biol. Chem.* **2003**, *278*, 15532.
16. Rella, M.; Rushworth, C. A.; Guy, J. L.; Turner, A. J.; Langer, T.; Jackson, R. M. *J. Chem. Inf. Model* **2006**, *46*, 708.
17. Huentelman, M. J.; Zubcevic, J.; Hernandez Prada, J. A.; Xiao, X.; Dimitrov, D. S.; Raizada, M. K.; Ostrov, D. A. *Hypertension* **2004**, *44*, 903.
18. Deaton, D. N.; Gao, E. N.; Graham, K. P.; Gross, J. W.; Miller, A. B.; Strelow, J. M. *Bioorg. Med. Chem. Lett.* **2008**, *18*, 732.
19. Hydrolyses were performed under an argon atmosphere. When hydrolyses were carried out with reactions open to the atmosphere, varying amounts of disulfide products were isolated, likely from aerobic oxidation. The enzyme assays contain a reducing agent, Tris-(2-chloroethyl)-phosphate (TCEP), to prevent oxidation of the thiols to disulfides during the assays. Dilutions of 10 mM stock solutions of the thiols **1a**–**1t** to final assay concentrations were done with 50% aqueous acetonitrile just prior to protease inhibition studies. Under these standard conditions, both the thiols and their corresponding disulfides showed enzyme inhibitory activity. Presumably, the disulfides were reduced to their corresponding thiols by TCEP during the pre-incubation period, before substrates were added. In contrast, if the assays were performed without TCEP, the disulfides were completely inactive, while the potencies of the thiols were attenuated, probably because of partial aerobic oxidation to their corresponding disulfides during the pre-incubation period.
20. Irvine, J. D.; Takahashi, L.; Lockhart, K.; Cheong, J.; Tolan, J. W.; Selick, H. E.; Grove, J. R. *J. Pharm. Sci.* **1999**, *88*, 28.
21. Lambert, M. H. In *Practical Application of Computer-Aided Drug Design*; Charifson, P. S., Ed.; Marcel Dekker: New York, NY, 1997; p 243.
22. The 'grow' algorithm within the MVP program was used to dock the inhibitor into the active site beginning from the carboxylic acid group.
23. Towler, P.; Staker, B.; Prasad, S. G.; Menon, S.; Tang, J.; Parsons, T.; Ryan, D.; Fisher, M.; Williams, D.; Dales, N. A.; Patane, M. A.; Pantoliano, M. W. *J. Biol. Chem.* **2004**, *279*, 17996.